Available online at www.sciencedirect.com
SCIENCE DIRECT
Polymer 46 (2005) 7301–7308
polymer
www.elsevier.com/locate/polymer

Modeling the elastomeric properties of stereoregular polypropylenes in nanocomposites with spherical fillers

Taner Z. Sen[a,b], Mohammed A. Sharaf[c], James E. Mark[d], Andrzej Kloczkowski[a,*]

[a]*L.H. Baker Center for Bioinformatics and Biological Statistics, Iowa State University, Ames, IA 50011-3020, USA*
[b]*Department of Biochemistry, Biophysics, and Molecular Biology, Iowa State University, Ames, IA 50011, USA*
[c]*Department of Chemistry, Helwan University, Cairo 11795, Egypt*
[d]*Department of Chemistry and the Polymer Research Center, The University of Cincinnati, Cincinnati, OH 45221-0172, USA*

Received 17 March 2005; received in revised form 20 May 2005; accepted 24 May 2005
Available online 1 July 2005

Abstract

The elastomeric properties of networks of stereoregular polypropylenes (PP) filled with spherical nanoparticles have been modeled in an attempt to obtain better insights into elastomer reinforcement. The polymers were either isotactic or syndiotactic PP in the amorphous state, and the simulations were based on rotational isomeric state (RIS) theory combined with the largest eigenvalue method for deriving conditional bond probabilities. Monte Carlo simulations gave distributions of the end-to-end distance of these chains in the presence of the particles, and these were used in the Mark–Curro theoretical approach to calculate values of the normalized stress, and the reduced stress (shear modulus) under uniaxial stretching. The simulations were calculated for PP chains having 100–200 skeletal bonds, for several temperatures from 481 to 650 K, and for varying filler particle sizes (up to 100 Å). The presence of the filler nanoparticles was found to influence chain conformations, frequently leading to significant chain extensions, which significantly affect the elastomeric properties of the nanocomposites.

Keywords: Stereoregular polypropylenes; Rotational isomeric state theory; Monte Carlo simulations

1. Introduction

Solid nanoparticles incorporated into elastomers substantially improve their mechanical properties, and are widely used for this purpose. In fact, this reinforcement phenomenon has been extensively used in many industrial applications to improve the mechanical properties of such materials for almost a century. Specifically, the addition of filler improves a wide range of properties, including the modulus at given strain, tensile strength, tear and abrasion resistance, resilience, and extensibility [1]. Experimental evidence indicates that the reinforcement depends on the size of filler particles, with maximum improvements obtained for very large particles of 10–100 nm in radius. Larger particles can actually weaken the polymer, instead of reinforcing it!

Although the reinforcement with fillers has been known and exploited for a very long time, its molecular origins are still not clear and there are many different, qualitative explanations of these phenomena. Particularly during the last decade, many theoretical and computational studies have been performed to elucidate the molecular mechanisms of filler reinforcement in nanocomposites. However, the nature of this reinforcement is still not well known, and there are still many controversies regarding molecular descriptions of reinforcement in filled elastomers in particular [2–18].

When polymer chains adsorb at a filler particle surface, covalent bonds are frequently formed in what is called chemisorption. Another factor that is closely related to the adsorption is the change in the distribution of end-to-end distance of polymer chains in the presence of filler particles. This 'excluded volume effect' imposed by the filler increases the non-Gaussian characteristics of polymer chains near the filler particles.

* Corresponding author. Tel.: +1 515 294 7261; fax: +1 515 294 3841.
E-mail address: kloczkow@iastate.edu (A. Kloczkowski).

0032-3861/$ - see front matter © 2005 Elsevier Ltd. All rights reserved.
doi:10.1016/j.polymer.2005.05.098

The first theoretical attempt to explain the dependence of filled elastomers on the concentration of filler was carried out many years ago by Guth and Gold [19]. These authors modified the Einstein viscosity equation for spherical particles in a viscous medium by adding quadratic term to account for interactions between particles, and obtained the equation

$$\eta = \eta_0(1 + 2.5\phi + 14.1\phi^2) \tag{1}$$

where η and η_0 are the viscosities for filled and the unfilled elastomer and ϕ is volume fraction of filler. Eq. (1) was later generalized by Guth to non-spherical particles [20]:

$$\eta = \eta_0(1 + 0.67\phi f + 1.62\phi^2 f^2) \tag{2}$$

where f is the shape factor used in the estimation of particle anisometry.

There are several other models of reinforcement in polymer composites [21], but most of these theories are not molecular. In fact, there is still a serious lack of a rigorous extension of the statistical theory of rubber elasticity to filled elastomers, in spite of their importance. Two exceptions are a statistical model of filled polymer networks (by Heinrich and Vilgis) based on the replica formalism [22], and a simple molecular model of filler reinforcement (formulated by Kloczkowski, Sharaf and Mark) [23–27]. In the latter approach, the filler particles change the distribution of the end-to-end distance of the polymer chains, due to the mentioned excluded volume of the filler and due to the adsorption of chains onto the filler surface. This leads to the change of elastic behavior of the polymer network. In this approach, calculations of the elastomeric properties of chains in unfilled networks and in filled networks was carried out using Monte Carlo rotational isomeric state simulations for single polymer chains. The simulations were performed for amorphous chains of polyethylene (PE) [23] and poly(dimethylsiloxane) (PDMS) [24] with various degrees of polymerization, and for different temperatures and different sizes of the filler particles.

In the present paper we extend these computations to filled networks of amorphous polypropylene (PP). PP is more difficult for theoretical study than is PE or PDMS, because of its asymmetric carbon atoms (that are absent in the symmetric chains of PE and PDMS). Because of this asymmetry there are stereoregular PP chains and stereoirregular PP chains, but the present study will focus on the isotactic and syndiotactic stereoregular forms. The main motivation of our paper is the study of the effect of tacticity on elastic properties of polymer chains, and answering the question if increase of the dimensions of the chains due to the filler particles (observed experimentally, and in our simulations for PE and PDMS) holds also for PP.

2. Methodology

The method employed is based on the Monte Carlo rotational isomeric state model [28,29] for obtaining distributions of the end-to-end distance for free polymer chains, and for chains attached at one end to a filler surface. These calculated distribution functions then enable the prediction of elastomeric properties of the chains within the framework of the Mark–Curro theory [30,31].

The distribution $P(r)$ of the end-to-end distance obtained by Monte Carlo simulation is directly related to the Helmholtz free energy $A(r)$ of a chain with the end-to-end distance r

$$A(r) = c - kT \ln P(r) \tag{3}$$

where c is a constant. The application of the 'three-chain model' [31] then gives the following expression for the elastic free energy change during the deformation of the network, as the function of elongation ratio α

$$\Delta A = \frac{\nu}{3}[A(r_0\alpha) + 2A(r_0\alpha^{-1/2}) - 3A(r_0)] \tag{4}$$

Here, ν is the number chains in the network and r_0 is the value of root-mean-square end-to-end vector of the network chains. The derivation of Eq. (4) utilizes the simplifying assumption of affine deformation of the network chains (their following the macroscopic deformation in a linear manner).

The nominal stress f^* defined as the elastic force at equilibrium per unit cross-sectional area of the sample in the undeformed state is

$$f^* = -T\left(\frac{\partial \Delta A}{\partial \alpha}\right)_T \tag{5}$$

Substitution of Eq. (4) into Eq. (5) then gives

$$f^* = -\frac{\nu kTr_0}{3}[G'(r_0\alpha) - \alpha^{-3/2}G'(r_0\alpha^{-1/2})] \tag{6}$$

where $G(r) = \ln P(r)$, and $G'(r)$ denotes the derivative $\mathrm{d}G/\mathrm{d}r$.

The most crucial step in our theory is the calculation of end-to-end distance distribution function for a rotational isomeric state model of the polymer chains using the RIS theory and the largest eigenvalue method for the required conditional probabilities. These analytically obtained probabilities are later used in a Monte Carlo algorithm generating representative polymer chains. Our method for stereoregular PP chains follows the methodology developed earlier by us for symmetric chains, such as PE and PDMS [23–27].

2.1. Derivation of conditional probabilities for polypropylene

The PP chain has a repeat unit with two skeletal bonds. The presence of an asymmetric center in a chain molecule

like PP causes a distinction between the handedness of the rotations around skeletal bonds. Because of this handedness, the frequencies of states corresponding to the left and right rotations differ.

For asymmetric vinyl chains $(–CHR–CH_2–)_x$ such as PP (with R being CH_3), we have two different statistical weight matrices corresponding to different stereochemical configurations. If the R groups are located in the front of the plane formed by the skeletal bonds of the fully extended chain, the corresponding carbon atoms are called d centers, while C atoms having R groups located behind this plane are called l centers [28]. Since any 180° rotation about the vertical axis of this plane changes d centers to l centers (and l centers to d centers) the stereochemical configuration of a given center is defined relative to its neighboring centers. Therefore, the pair ll is equivalent to dd due to symmetry, but differs from the pair ld (or dl), since such a symmetry operation cannot be applied. Such stereochemical neighbor pairs are called dyads [28].

For the dd dyad the two statistical weight matrices are [28,32]: $\mathbf{U}'_{\mathrm{d}}$ corresponding to the CHR–CH_2 bond, and $\mathbf{U}''_{\mathrm{d}}$ corresponding to the CH_2–CHR bond.

The statistical weight matrices for the ll dyad are $\mathbf{U}'_{\mathrm{l}}$ and $\mathbf{U}''_{\mathrm{ll}}$ that are equivalent to $(\mathbf{U}'_{\mathrm{d}})^T$ and $(\mathbf{U}''_{\mathrm{d}})^T$ [28]. For the syndiotactic chains the statistical weight matrices are $\mathbf{U}''_{\mathrm{dl}}$ and $\mathbf{U}''_{\mathrm{ld}}$ [28]. All these statistical weight matrices depend on four RIS theory parameters η, τ, ω and τ^* [28]. More details about these matrices and explicit expressions for $\mathbf{U}'_{\mathrm{l}}$, $\mathbf{U}''_{\mathrm{ll}}$, $\mathbf{U}''_{\mathrm{d}}$, $\mathbf{U}''_{\mathrm{dd}}$, $\mathbf{U}''_{\mathrm{dl}}$ and $\mathbf{U}''_{\mathrm{ld}}$ in terms of the parameters η, τ, ω and τ^* are provided in Ref. [28]. For the isotactic PP, these matrices repeat regularly in the sequence $(\mathbf{U}'_{\mathrm{d}}\,\mathbf{U}''_{\mathrm{d}})_x$ where x is the number of dyads, so one may combine them into a single matrix [28,32]:

$$\mathbf{U}^{(2)}_{\mathrm{isotactic}} = \mathbf{U}'_{\mathrm{d}}\mathbf{U}''_{\mathrm{dd}} \tag{7}$$

The above equation applies to dd dyads, and for ll dyads the corresponding equations have a similar form. For simplicity we will use a shorter notations $\mathbf{U}_a$ and $\mathbf{U}_b$ and $\mathbf{U}^{(2)} = \mathbf{U}_a\,\mathbf{U}_b$, which describe both dd and ll dyads. In the case of syndiotactic chains, however, matrix $U^{(2)}$ equals $\mathbf{U}'_{\mathrm{d}}\mathbf{U}'_{\mathrm{dl}}\mathbf{Q}$, where

$$\mathbf{Q} = \begin{bmatrix} 1 & 0 & 0 \\ 0 & 0 & 1 \\ 0 & 1 & 0 \end{bmatrix}$$

is the matrix that interchanges rows and columns corresponding to the states g^+ and g^- [28,32].

We note that there are several different rotational isomeric state models of PP that differ in the number of rotational states assumed [33–37]. The first model, proposed by Flory and coworkers, was based on three rotational states [33]. There are more accurate models of PP involving five rotational states developed by Suter and Flory [37], or even nine states (Boyd and Breitling) [36]. The three-state model with proper parameterization [35] has, however, been successfully used for calculations of various properties of PP chains. In the present work we use the simplest three-state RIS model proposed by Abe, Tonelli, and Flory in 1970 [33]. Values of the parameters used were $\eta = 1.0$, $\tau = 0.5$, $\omega = 0.05$, and $\tau^* = 1.0$, which correspond to the temperature 481 K.

The largest eigenvalue method developed recently for stereoregular vinyl chains by Kloczkowski, Sen and Sharaf [38] leads to the following expression for the bond probabilities:

$$P_{a,\xi\eta} = \frac{1}{\lambda_1} B_{1\xi} u_{a,\xi\eta} [A_{11} u_{b,\eta 1} + A_{21} u_{b,\eta 2} + A_{31} u_{b,\eta 3}] \tag{8}$$

and

$$P_{b,\xi\eta} = \frac{1}{\lambda_1} u_{b,\xi\eta} A_{\eta 1} [B_{11} u_{a,1\xi} + B_{12} u_{a,2\xi} + B_{13} u_{a,3\xi}] \tag{9}$$

where A_{ii} and B_{ij} are ij-th elements of matrices $\mathbf{A}$ and $\mathbf{B} = \mathbf{A}^{-1}$ obtained from the diagonalization of the matrix $U^{(2)}$

$$\mathbf{B}\mathbf{U}^{(2)}\mathbf{A} = \mathbf{\Lambda} \tag{10}$$

Here, $\mathbf{\Lambda}$ is the matrix containing eigenvalues on the diagonal and zeros off-diagonal and λ_1 is the largest eigenvalue; $u_{a,\xi\eta}$ (or $u_{b,\xi\eta}$) are elements of the matrices $\mathbf{U}_a$ and $\mathbf{U}_b$.

It is now straightforward to obtain the conditional a priori bond pair probabilities that the bond i is in state η given that bond $i-1$ is in state ζ:

$$q_{a,\xi\eta} = \frac{P_{a,\xi\eta}}{P_{a,\xi}} \tag{11}$$

$$q_{b,\xi\eta} = \frac{P_{b,\xi\eta}}{P_{b,\xi}} \tag{12}$$

where $P_{a,\xi} = \sum_{\eta=1}^{3} P_{a,\xi\eta}$ and $P_{b,\xi} = \sum_{\eta=1}^{3} P_{b,\xi\eta}$ are single bond probabilities. The conditional probabilities can be used for a very efficient Monte Carlo generation of long polymer chains, we should however note that this involves an approximation, that may effect results, especially for bonds close to chain ends.

2.2. Monte Carlo chain generations

The generation of a representative chain consisted of finding a sequence of rotation angles, i.e. sequences of *trans* and *gauche* conformations. For the case of PE, the first bond of the PE chain was assumed to be in the *trans* conformation [23]. Random numbers were then generated for each of the remaining skeletal bonds. Specifically for the second bond, $0 \le r < q_{\zeta 1}$ was taken to specify a *trans* conformation, $q_{\zeta 1} \le r < (q_{\zeta 1} + q_{\zeta 2})$ was taken to specify a *gauche*+ conformation, and $(q_{\zeta 1} + q_{\zeta 2}) \le r < 1$ a *gauche*− conformation. The next bond was then positioned using the same algorithm, but with the row index ζ of the elements q determined by the conformation of the previous bond. The process was repeated until the entire conformation of a PE

chain of n bonds was generated. The Monte Carlo generation of PP was very similar, but instead of a single conditional probability matrix, there were two alternating matrices $\mathbf{Q}_a$ and $\mathbf{Q}_b$. The conditional probabilities $q_{\zeta\eta,a}$ and $q_{\zeta\eta,b}$ were therefore also alternated during the generation of the chain. It was also necessary to make a trivial assumption with regard to the first carbon atom of the PP chain, and this was that the group was of the type –CH_2–. Large numbers of Monte Carlo chains (N=500,000) were thus generated to ensure an adequate statistical sample. For each chain, the end-to-end vector $\mathbf{r}$ was calculated using the formula [28]:

$$\mathbf{r} = (\mathbf{E} + \mathbf{T}_1 + \mathbf{T}_1\mathbf{T}_2 + \cdots + \mathbf{T}_1\mathbf{T}_2 \ldots \mathbf{T}_{n-1})\mathbf{l} \tag{13}$$

Here, $\mathbf{E}$ is the unit matrix of order 3, $\mathbf{l}$ is the bond vector col(l_0,0,0), where l_0 is the equilibrium bond length (l_0= 1.54 Å for the C–C bonds). The rotational matrices T_i($1 < I < n-1$) are given by [28]

$$\mathbf{T}_i = \begin{bmatrix} \cos\theta_i & \sin\theta_i & 0 \\ \sin\theta_i\cos\varphi_i & -\cos\theta_i\cos\varphi_i & \sin\varphi_i \\ \sin\theta_i\sin\varphi_i & -\cos\theta_i\sin\varphi_i & -\cos\varphi_i \end{bmatrix} \tag{14}$$

and the complement bond angles θ_i is 68.0°. The rotational angles are 0, 120, and −120° for conformations t, $g+$, and $g-$. It was assumed that the first bond between the filler and the chain is perpendicular to the surface of the sphere and is contacting the spherical particle. The assumption is that the first bond is perpendicular is arbitrary but trivial, and simplifies the model. During the process of chain generation, each bond of the chain was tested for overlapping with the filler particle. If any bond penetrated the particle surface the whole chain conformation was rejected (Fig. 1). The resulting acceptable values of r were then placed into a histogram to produce the desired end-to-end distance probability distribution function $P(r/nl_0)$.

We constructed a histogram with 20 equally spaced intervals over the allowed range $(0 < r/nl_0) < 1$, since previous studies showed that this choice was the most suitable for obtaining probability distribution functions [39]. This distribution function was obtained by accumulating the numbers of Monte Carlo chains with end-to-end distance within various space intervals, and dividing these numbers by the total number of the Monte Carlo Chains, N. The function $P(r/nl_0)$ was smoothed using the IMSL cubic spline subroutine CSINT. The smoothing procedure is necessary for the proper calculation of the stress–strain isotherms from the Monte Carlo histogram [39].

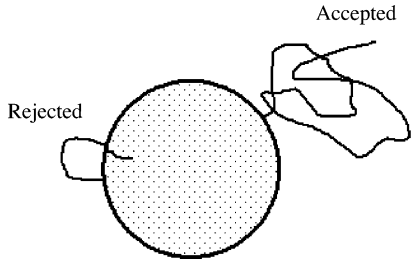

Fig. 1. Schematic representation of the filler system employed in this study. A spherical particle is positioned in the middle of the coordinate system, and the chain generation started on its surface. Chain conformations that trespassed on the particle were rejected, and statistical calculations were performed on the remaining acceptable conformations.

2.3. Modeling of uniaxial elongation

These results can be used directly in the Mark–Curro method to calculate the elastomeric network properties of any non-Gaussian chains from the distribution functions $P(r)$ [30,31]. As already described, $P(r)$ is directly related to the Helmholtz free energy $A(r)$ of a chain having the end-to-end distance r (Eq. (3)). This equation can be applied to the case of elongations in which the chains respond affinely to the macroscopic deformation. The macroscopic deformation λ along the direction i is defined as

$$\lambda_i = \frac{L_{ti}}{L_{0i}} \tag{15}$$

Here L_{0i} is the length of the sample in the direction i (i= x,y,z) in the unfilled reference state and L_{ti} is its value in the filled network during the experiment. Assuming an affine deformation, L_{0i} and L_{ti} are both related to the i components of the end-to-end vector of the chains. The three main-axis deformation tensor components are related to the volume at the start of the experiment V, and the reference volume V_0 of the isotropic unfilled network by

$$\lambda_1\lambda_2\lambda_3 = \frac{V}{V_0} \tag{16}$$

Since in this study anisotropy is induced only along the direction of the deformation, it follows that two of the three terms are equivalent. As would be expected, $V \neq V_0$ due to anisotropy of the polymer chain induced by the filler particles. The deformation ratio α_i relative to the dimension L_{ti} during stretching is given for the case of isotropic deformation by

$$\alpha_i = \left(\frac{V}{V_0}\right)^{-1/3}\lambda_i \tag{17}$$

for anisotropic deformations

$$\alpha_i = (\lambda_{ti})^{-1}\lambda_t \tag{18}$$

Incompressibility of the network is assumed, so the volume V remains constant after the stress is applied. When the deformation is applied along the draw direction, for example the z-axis,

$$\lambda_z = (\lambda_{zt})\alpha \quad \lambda_x = \lambda_y = (\lambda_{xt})\alpha^{-1/2} \tag{19}$$

Within these approximations, the three-chain model leads to the general expression for the elastic free energy change during deformation given by Eq. (4). [30,31]:

The nominal stress f^* defined as the elastic force at equilibrium per unit cross-sectional area of the sample in the

undeformed state [40] is given by Eq. (6). The modulus (or 'reduced stress') is defined by [40]

$$[f^*] = \frac{f^*}{\alpha - \alpha^{-2}} \tag{20}$$

and is often fitted to the Mooney-Rivlin semi-empirical formula [40]

$$[f^*] = 2C_1 + 2C_2\alpha^{-1} \tag{21}$$

where C_1 and C_2 are constants independent of deformation α. Some of the present results obtained will be presented in this form.

The numerical calculations were performed for PP chains having lengths 100–200 skeletal bonds between cross-links, for spherical particles radii ranging from 0 to 100 Å, and for temperatures from 481 to 650 K.

3. Results

3.1. The effects of chain length

Fig. 2 shows the normalized end-to-end distance distribution for isotactic PP at chain lengths of 100, 150, and 200 bonds, at 481 K, in the presence of fillers of size 10 Å. The normalization was performed by dividing the end-to-end distance by the maximum chain extension, where n is the number of bonds, and l is the bond length. The distributions show a Gaussian character. With increasing chain length, the distribution becomes narrower and its peak shifted towards smaller values according to the theory of the freely jointed chain model [28]. Fig. 2 shows that the presence of the filler particle leads to the attrition of shorter chains as a result of steric clashes and shifts the distribution to the right.

Fig. 3 shows the end-to-end chain distribution of syndiotactic PP at $T=481$ K, 10 Å for various chain lengths. We again observe that with increasing chain length, the distribution becomes narrower, and the peak position shifts to lower values. However, there is striking difference between the distribution of isotactic and syndiotactic PP: at the same chain length, the peak position for syndiotactic PP is greater than that of isotactic PP. This difference arises since syndiotactic PP is more likely to assume *trans* conformations than is isotactic PP.

Fig. 4 shows the nominal stress for syndiotactic PP under the same conditions as in Figs. 2 and 3. The calculations were performed for chains of 100, 150, and 200 bonds. At the beginning of the elongation, the chains of different lengths followed the same linear curve corresponding to the elastic region. The plastic region appears earlier for chains of 100 bonds as compared to the chains of 150 or 200 bonds, which basically follow almost the same pattern throughout the elongation. Chains of 100 bonds require greater stresses to be elongated once this critical point is reached. This need for higher stresses can be explained in light of end-to-end distance distribution in Fig. 3: since the chains of 100 bonds are already more extended than the chains of 150 and 200 bonds, the amount of additional elongation they can endure until the end of elastic region is more limited. Once the plastic region is reached, the stress development gains a non-linear character as elongation is continued.

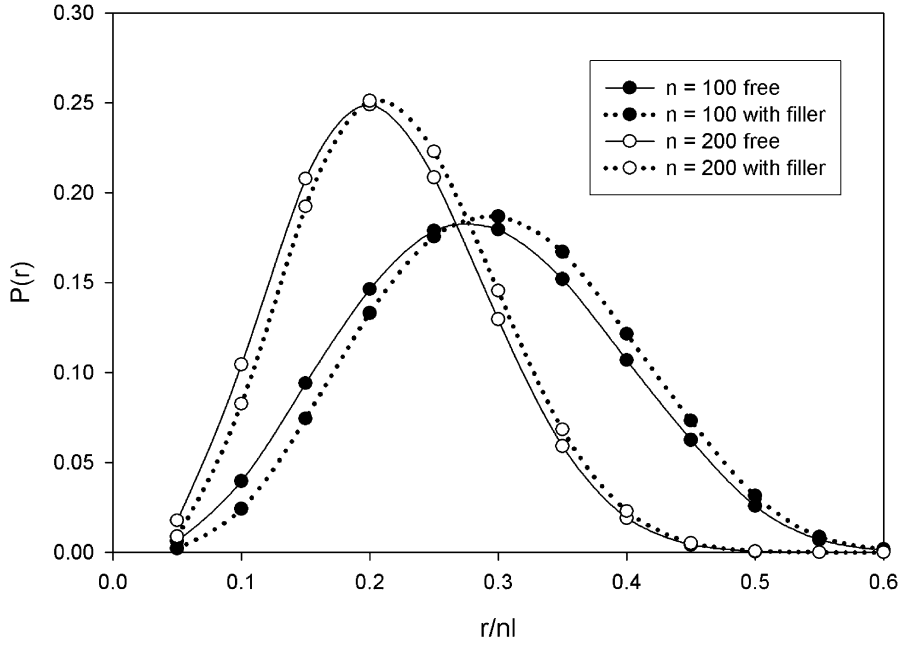

Fig. 2. The normalized end-to-end distance distribution for isotactic PP as a function of chain length, at $T=481$ K, with a filler radius of 10 Å. In order to emphasize the effect of the filler, the distributions when no filler is present are also plotted.

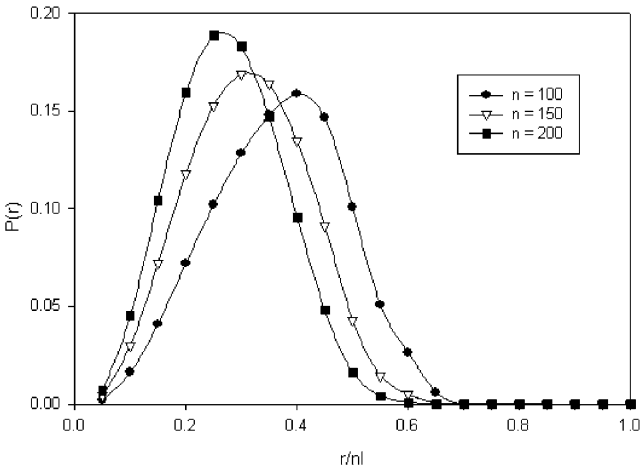

Fig. 3. The normalized end-to-end distance distribution for syndiotactic PP as a function of chain length, with $T=481$ K, with a filler radius of 10 Å.

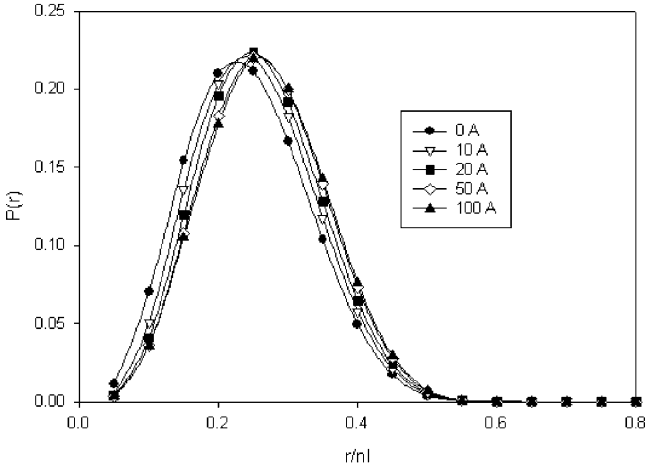

Fig. 5. The normalized end-to-end distance distribution of isotactic PP for various filler sizes, for chains of 150 bonds, at $T=481$ K.

3.2. The effects of filler size

Fig. 5 shows the normalized end-to-end-distance distribution of isotactic PP for filler sizes up to 100 Å. The curves show that filler size did not affect the distribution shape, but larger fillers slightly shifted the distribution to larger distances. This shift can also be seen in the simulations of filled PE and PDMS reported in previous studies [23,24]. This effect originates solely due to the filler geometry. An increase in the filler radius promotes slightly larger values of *r/nl* since chains can now go around the filler.

For large diameters of the filler particle, relative to the size of the chain, the distribution function of the end-to-end distance of polymer becomes weakly dependent on the diameter of the sphere, approaching the limiting distribution of a chain attached to a flat surface (saturation effect).

Fig. 6 clearly shows the effects of end-to-end distance distribution on the nominal stress as a function of stretching ratio. Since the chains are already extended at large filler sizes, the stress necessary for stretching a chain that is already extended is higher than that of a less extended chain. The effect of saturation can again be seen by comparing the nominal stress curves for the cases involving 50 and 100 Å.

The initial reduced stresses in Fig. 7 agree with previous results. The initial shear moduli increased with increasing filler size due to the degree of chain extension before elongation. At the beginning of the elongation, the moduli stayed almost constant. However, in later stages of stretching, the modulus curves reach an upturn at a critical stretch ratio, which is independent of filler size. After this point, the chain stretching acquires a non-Gaussian character.

3.3. The effects of temperature

Fig. 8 illustrates the normalized end-to-end distance distribution for syndiotactic PP at temperatures ranging from 481 to 650 K.

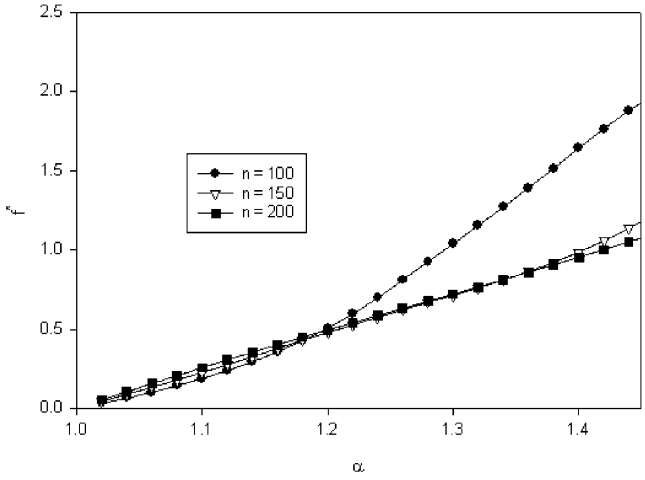

Fig. 4. The nominal stress for syndiotactic PP as a function of stretch ratio for different chain lengths, at $T=481$ K, at a filler radius of 10 Å.

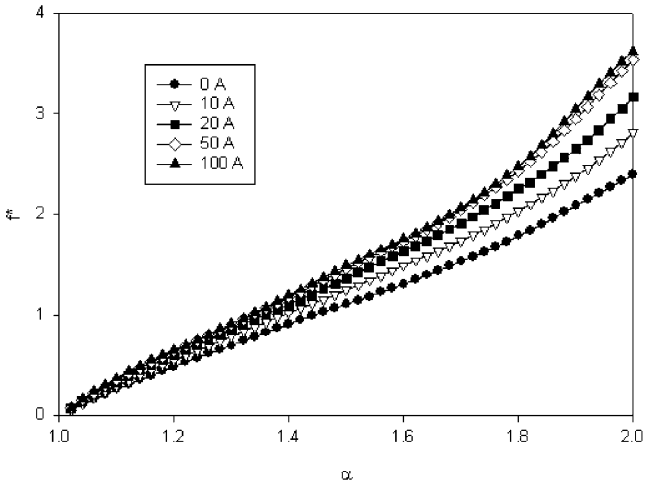

Fig. 6. The nominal stress for isotactic PP as a function of stretch ratio for various filler sizes, for chains of 150 bonds, at $T=481$ K.

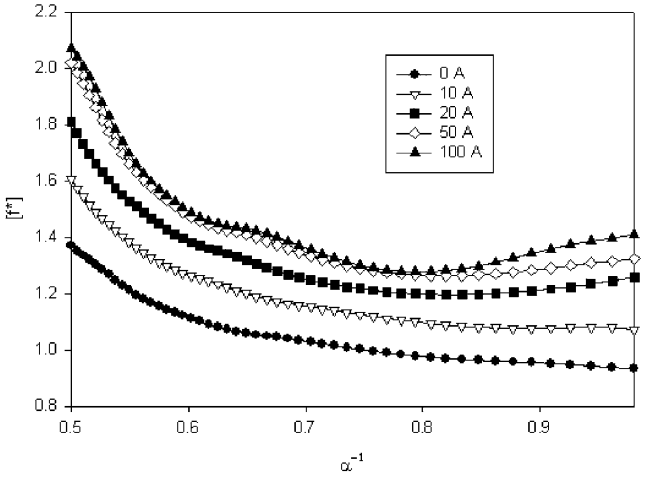

Fig. 7. The reduced stress (shear modulus) for isotactic PP as a function of stretch ratio for various filler sizes for chains of 150 bonds at $T=481$ K.

With increasing temperatures, the distribution curve became narrower, and the peak was shifted to lower end-to-end distances. At low temperatures, the low-energy trans bonds are preferred, and therefore larger end-to-end distances were reached. At high temperatures, however, more higher-energy conformational states were available to the bonds, an outcome which shifted the distribution curves and populated it with shorter chains.

Fig. 9 again shows the effect of pre-extended chains in the extension. With increasing temperatures, fewer and fewer bonds populate *trans* conformations, and subsequently, less stress is necessary for chain elongation.

The end of the elastic region can be clearly seen in Fig. 10 where the reduced stress showed an upturn during elongation. This critical transition point was difficult to identify from these results, since the variance may well be caused by computational errors introduced by derivative calculations. However, the reduced stress curves clearly agreed with the results presented in Figs. 8 and 9.

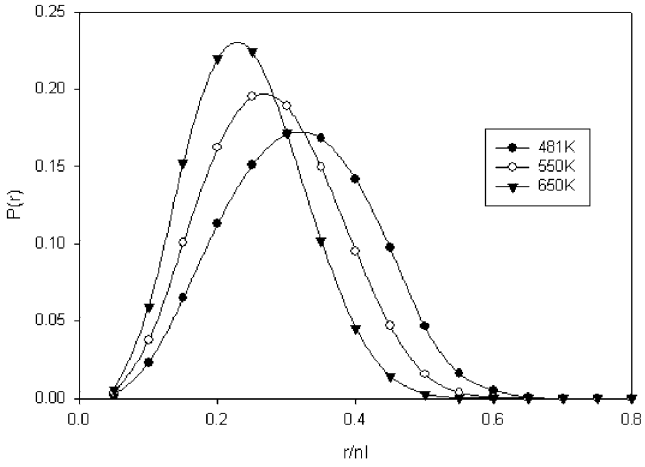

Fig. 8. The normalized end-to-end distance distribution of syndiotactic PP at various temperatures, for chains of 150 bonds, with a filler radius of 10 Å.

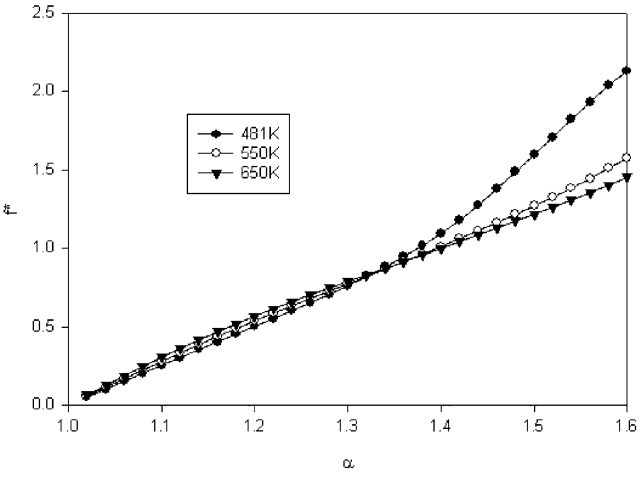

Fig. 9. The nominal stress for syndiotactic PP as a function of elongation at various temperatures for chains of 150 bonds, with a filler radius of 10 Å.

4. Conclusions

Conformational aspects and deformation characteristics of isotactic and syndiotactic polypropylene filled with spherical nanoparticles were successfully elucidated. Chains having from 100 to 200 skeletal bonds were generated on the surface of a filler particle at temperatures ranging from 481 to 650 K. This clarified the effects of presence of the filler particles, for radii up to 100 Å. Increasing the chain length or decreasing the temperature were found to affect the chain properties similarly: the normalized mean end-to-end distance increased, in turn shrinking the elastic region during deformation. Increasing the filler size also increased the normalized mean end-to-end distance slightly.

Also clarified were the effects of PP tacticity. Since syndiotactic PP more readily assumes the trans conformation, the normalized mean end-to-end distance is greater than that of isotactic PP. This difference affects the

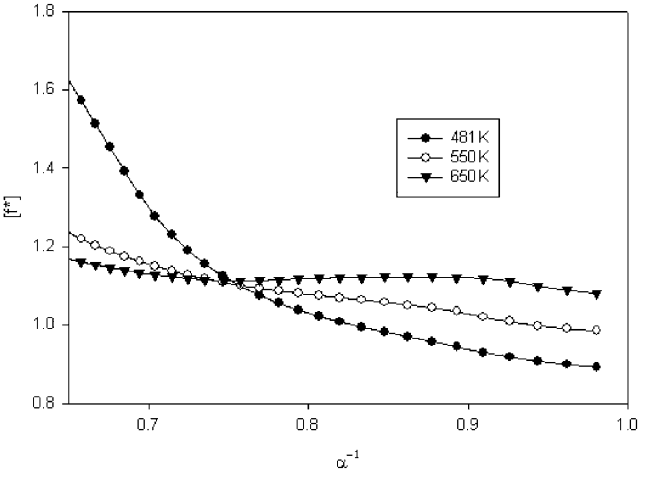

Fig. 10. The reduced stress for syndiotactic PP as a function of elongation at various temperatures for chains of 150 bonds, with a filler radius of 10 Å.

deformation, since the syndiotactic chains reach the end of the elastic region at lower elongations than do the isotactic chains.

The present results showed increases of the dimensions of the chains due to the filler particles, in agreement with results reported in earlier papers [23–27]. Very relevant here is the fact that such increases in dimensions have been observed in experimental scattering studies on PDMS by Nakatani et al. [41,42]. It has therefore become increasingly important to understand some simulations that have led to the opposite conclusion, namely that filler particles should decrease the dimensions of chains in filled elastomers [3,5]. Indeed, our new simulation results with denser polymer-filler systems, (where instead of studying a polymer chain attached to a single filler particle, we study interaction of a chain with multiple filler particles) suggest that the filler particles increase chain dimensions only up to a certain critical filler size; above this critical filler size, the filler particles decrease chain dimensions. This problem in denser polymer-filler composites will be studied in more detail in our future work [43].

Acknowledgements

It is a pleasure to acknowledge the financial support provided JEM by the National Science Foundation through Grant DMR-0314760 (Polymers Program, Division of Materials Research). AK acknowledges the financial support provided by the NIH grant 1R01GM072014-01.

References

[1] Rigbi Z. Adv Polym Sci 1980;36:21–68.
[2] Hooper JB, McCoy JD, Curro JG. J Chem Phys 2000;112:3090–3.
[3] Vacatello M. Macromolecules 2001;34:1946–52.
[4] Vacatello M. Macromol Theory Simul 2002;11:757–65.
[5] Vacatello M. Macromolecules 2002;35:8191–3.
[6] Heinrich G, Kluppel M, Vilgis TA. Curr Opin Solid State Mater Sci 2002;6:195–203.
[7] Gersappe D. Phys Rev Lett 2002;89. 58301-1–58301-4.
[8] Fuchs M, Schweizer KS. J Phys Condens Matter 2002;14:R239–69.
[9] Starr FW, Schroeder TB, Glotzer SC. Macromolecules 2002;35:4481–92.
[10] Ozmusul MS, Picu RC. Polymer 2002;43:4657–65.
[11] Picu RC, Ozmusul MS. J Chem Phys 2003;118:11239–48.
[12] Schmidt G, Malwitz MM. Curr Opin Colloid Interf Sci 2003;8:103–8.
[13] Vacatello M. Macromol Theory Simul 2003;12:86–91.
[14] Vacatello M. Macromolecules 2003;36:3411–6.
[15] Barbier D, Brown D, Grillet AC, Neyertz S. Macromolecules 2004;37:4695–710.
[16] Doxastakis M, Chen YL, Guzman O, de Pablo JJ. J Chem Phys 2004;120:9335–42.
[17] Vacatello M. Macromol Theory Simul 2004;13:30–5.
[18] Hooper JB, Schweizer KS, Desai TG, Koshy R, Keblinski P. J Chem Phys 2004;121:6986–97.
[19] Guth E, Gold O. Phys Rev 1938;53:322.
[20] Guth E. J Appl Phys 1945;16:20–5.
[21] Ahmed S, Jones FR. J Mater Sci 1990;25:4933–42.
[22] Heinrich G, Vilgis TA. Macromolecules 1993;26:1109–19.
[23] Kloczkowski A, Sharaf MA, Mark JE. Comp Polym Sci 1993;3:39–45.
[24] Kloczkowski A, Sharaf MA, Mark JE. Chem Eng Sci 1994;49:2889–97.
[25] Sharaf MA, Kloczkowski A, Mark JE. Comp Theory Polym Sci 2001;11:251–62.
[26] Sharaf MA, Mark JE. Polymer 2004;45:3943–52.
[27] Yuan QW, Kloczkowski A, Mark JE, Sharaf MA. J Polym Sci, Part B-Polym Phys 1996;34:1647–57.
[28] Flory PJ. Statistical mechanics of chain molecules. New York: Wiley-Interscience; 1969.
[29] Mattice WL, Suter UW. Conformational theory of large molecules. The rotational isomeric state model in macromolecular systems. New York: Wiley; 1994.
[30] Curro JG, Mark JE. J Chem Phys 1984;80:4521–5.
[31] Mark JE, Curro JG. J Chem Phys 1983;79:5705–9.
[32] Flory PJ, Mark JE, Abe A. J Am Chem 1966;88:639–50.
[33] Abe A, Tonelli AE, Flory PJ. Macromolecules 1970;3:294–303.
[34] Akten ED, Mattice WL, Suter UW. Simulation methods for polymers. New York: Marcel Dekker; 2004, pp. 89-107.
[35] Biskup U, Cantow HJ. Macromolecules 1972;5:546–50.
[36] Boyd RH, Breitling SM. Macromolecules 1972;5:279–86.
[37] Suter UW, Flory PJ. Macromolecules 1975;8:765–76.
[38] Kloczkowski A, Sen TZ, Sharaf MA. Polymer 2005;46:4373–83.
[39] DeBolt LC, Mark JE. J Polym Sci, Part B: Polym Phys 1988;26:865–74.
[40] Erman B, Mark JE. Rubberlike elasticity. A molecular primer. New York: Wiley-Interscience; 1988.
[41] Nakatani AI, Chen W, Schmidt RG, Gordon GV, Han CC. Polymer 2001;42:3713–22.
[42] Nakatani AI, Chen W, Schmidt RG, Gordon GV, Han CC. Int J Thermophys 2002;23:199–209.
[43] Mark JE, Abou-Hussein R, Sen TZ, Kloczkowski A, Sharaf MA. Some simulations on filler reinforcement in polymers. Polymer, submitted.